



A new spacecraft mission concept combining the first exploration of the Centaurs and an astrophysical space telescope for the outer solar system

Kelsi N. Singer^{a,*}, S. Alan Stern^a, John Elliott^b, Reza R. Karimi^b, Daniel Stern^b, Arthur B. Chimelewski^b, Michael J. Fong^b, John Andrews^a, William F. Bottke^a, Catherine B. Olkin^a, Paul Propster^b, Sam W. Thurman^b

^a Southwest Research Institute, Boulder, CO, 80302, USA

^b Jet Propulsion Laboratory, California Institute of Technology, Pasadena, CA, 91109, USA

ABSTRACT

We present a concept study for a distinctive robotic spacecraft mission that combines both the exploration of a never-before-visited class of planetary bodies and cutting-edge astrophysical investigations. The planetary targets are a class of objects called Centaurs that have relatively recently escaped from the Kuiper Belt and currently orbit closer to the Sun among the giant planets. We developed a trajectory that would visit several Centaurs, including the second largest known Centaur, 2060 Chiron, which displays enigmatic coma activity at large heliocentric distances and orbiting ring or dust structures. This concept takes advantage of the cruise times between planetary encounters to conduct nearly continuous astrophysical observations at wavelengths that are not accessible by ground-based facilities. Additionally, ride-along cubesats included aboard can be deployed at different points in the mission to perform various experiments or observations. This mission concept achieves its objectives with solar power (MegaFlex arrays), no new technology development, and within the approximate budget of a NASA New Frontiers class mission. The mission design accomplishes its objectives using solar electric propulsion and the recently developed NASA Evolutionary Xenon Thruster (NEXT) ion engines.

1. Introduction and scientific rationale

We have developed a spacecraft mission concept with a novel combination of both planetary and astrophysical science goals, for a cost similar to a New Frontiers class NASA mission. This mission will visit a class of objects known as Centaurs, take astronomical observations en route, and also carry cubesats to be utilized for various purposes during its flight. Both the planetary and astrophysical objectives fill key scientific knowledge gaps that cannot be achieved by ground-based assets. We performed trajectory analysis, payload and other trade studies, and systems engineering analysis to develop a working mission concept at a maturity level similar to that of a pre-phase A study for a NASA mission call. However, specific payload instruments have not been selected, and therefore some scientific and other trade studies are left for future work.

1.1. Why visit Centaurs?

The outer solar system provides a scientific cornucopia with valuable information about the origin and evolution of planetary bodies. In particular, Kuiper Belt Objects (KBOs), which primarily reside beyond the orbit of Neptune, are a “Rosetta Stone” for information about the

early stages of the solar system and the building blocks of outer planets (e.g., NRC, 2011; Peixinho et al., 2020; Sicardy et al., 2020). Some KBOs from the scattered-disk subpopulation become gravitationally perturbed onto orbits closer to the Sun (Fig. 1), and then become Centaurs (e.g., Gomes et al., 2008; Nesvorný et al., 2019). Centaurs orbit among the giant planets Jupiter, Saturn, Uranus, and Neptune, and therefore have relatively short dynamical lifetimes because of continued gravitational perturbations by these giant planets (e.g., Duncan and Levison, 1997). The typical time a Centaur spends among the giant planets is 10^5 – 10^7 years (Gladman et al., 2001; Fernández et al., 2018) before they are ejected from this region or collide with a giant planet. Thus, we know that any extant Centaurs have arrived relatively recently from the Kuiper Belt. Centaurs therefore represent a closer and more accessible opportunity for spacecraft missions to extend our knowledge about distant Kuiper Belt Objects and through them, the building blocks of the outer planets.

The name “Centaurs” came about because the first few objects discovered in this population appeared to display aspects of both asteroids and comets. It is now known that some have unusual and unexplained coma activity, and rings have been discovered around larger Centaurs (Braga-Ribas et al., 2014; Ortiz et al., 2015; Ruprecht et al.,

* Corresponding author.

E-mail address: ksinger@boulder.swri.edu (K.N. Singer).

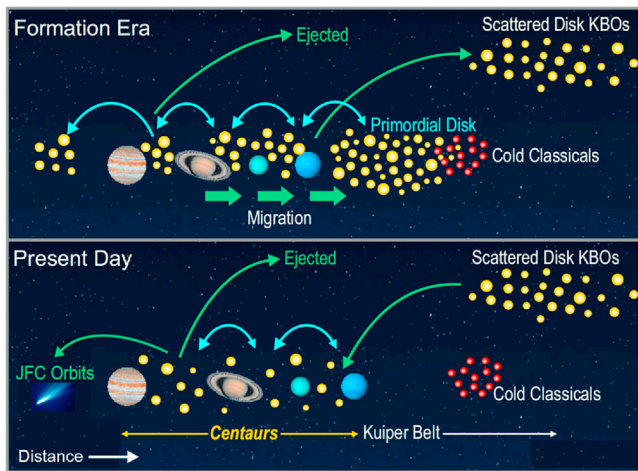


Fig. 1. Schematic of the rearrangement of the solar system that initially led to the scattered disk of the Kuiper belt, and the modern era evolution of scattered disk objects into Centaurs. Centaurs have short dynamical lifetimes in the giant planet region, and are subsequently ejected out of this region. Some Centaurs become Jupiter-family comets. Light blue, double-headed arrows indicate ongoing mixing of objects from locations under the gravitational influence of the giant planets. Green, single-headed arrows indicate when objects are transferred to significantly different populations outside of the giant planet region or ejected from the solar system.

2015; Fernández et al., 2018). Centaurs are also known to be active (i.e., ejecting material off of their surfaces) at much larger heliocentric distances than most Jupiter-family (i.e., short period) comets and their activity is not obviously correlated with heliocentric distance (e.g., they do not become more active only when they are closer to the Sun). Centaurs also represent a transition state between KBOs and Jupiter-family comets (e.g., Fernández et al., 2018), and some Centaurs are pushed from the giant planet region into closer orbits, while others are ejected back out beyond the giant planets.

Some Centaurs are quite large, similar in size the second largest known asteroid (4 Vesta) and the largest known trojan asteroid (624 Hektor). The largest two known Centaurs are 10199 Chariklo at ~250 km in diameter and 2060 Chiron at ~220 km in diameter (Fornasier et al., 2013). This mission would be the first to explore Centaurs and chose to focus on Chiron (Fig. 2) as its main exploration target for several reasons.

First, previous studies of Chiron have revealed it to be an active and unique mini-planet. Chiron frequently shows a coma even at its relatively large heliocentric distance (Luu and Jewitt, 1990; Bus et al., 1991; Womack and Stern, 1999; Romon-Martin et al., 2003) and stellar occultations have revealed structures off of the surface that are either dense orbiting rings or dust structures (Elliot et al., 1995; Bus et al., 1996; Ortiz et al., 2015; Ruprecht et al., 2015; Sickafoose et al., 2020). The coma activity generally occurs as discrete outbursts. Beyond 5 AU the sublimation of water ice cannot be the cause of activity. CO gas or N₂⁺ have been detected in some active Centaurs (Crovisier et al., 1995; Womack and Stern, 1999; Ivanova et al., 2015; Drahus et al., 2017; Wierzbach et al., 2017). Some researchers have thus concluded Centaur coma activity is due to sublimation of supervolatiles like CO, CH₄, O₂, or N₂ (e.g., Senay and Jewitt, 1994; Gunnarsson et al., 2008), while others have suggested processes like the exothermic conversion of amorphous to crystalline H₂O, impacts, thermal fracture, or space plasma interactions drive the activity (e.g., Prialnik et al., 1995; Enzian et al., 1997; Jewitt, 2009; Meech et al., 2009; Jewitt et al., 2019). Distant coma activity and rings around small bodies are a puzzling phenomenon never before explored by spacecraft.

Second, Chiron's orbit and location provide other scientific and technical advantages. Chiron has a perihelion distance of 8.4 AU making

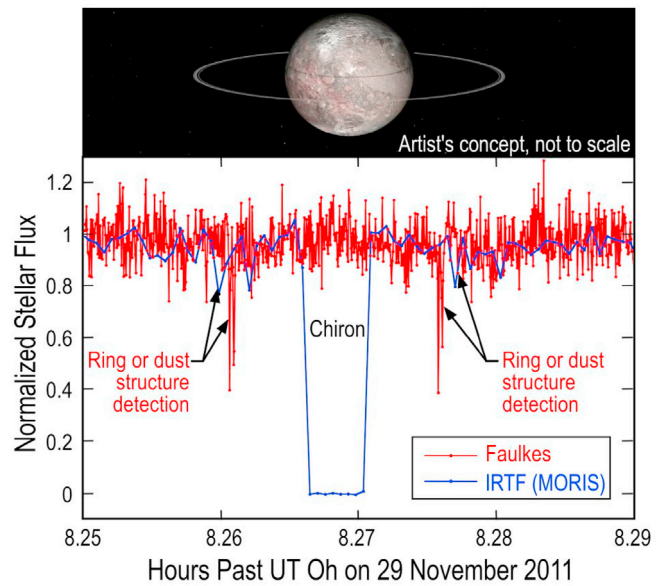


Fig. 2. Chiron is a large Centaur explored in this mission concept. Chiron has displayed evidence for orbiting rings or other dust structures in multiple stellar occultations. This 2011 stellar occultation (bottom panel) showed evidence of symmetric opacity structures with significant optical depths. Upper artistic concept of Chiron courtesy Dan Durda; lower figure modified from Ruprecht et al. (2015).

it accessible with solar power (see section 3.3.) and it also has an inclination of just ~7°, making easier to reach while also exploring other Centaurs or primitive objects on the way (compared with some other large Centaurs like Chariklo that have higher inclinations). For comparison, the *New Horizons* mission to explore the Kuiper Belt flew by the Pluto system at 32.9 AU (Stern et al., 2015), and the small KBO Arrokoth at 43.3 AU (Stern et al., 2019), requiring radioisotope power. We did not choose Chariklo as a target because its perihelion is greater than 13 AU and its orbital inclination is 23.4° (which means it is often far out of the ecliptic for several decades at a time), making a solar-powered mission and encounters with other Centaurs on the same trajectory difficult.

Multiple National Research Council (NRC) reports over the past 15 years have called for Centaur and KBO exploration. For example, the 2003 Planetary Decadal Survey (NRC, 2003) called for sending a “flyby reconnaissance spacecraft equipped with imaging, imaging spectroscopy, radio science, and, potentially, other instruments to make the first explorations ... of a Centaur (a mission that) has deep ties to understanding the origins of primitive bodies.” The 2008 NRC New Opportunities for Solar System Exploration (NOSSE) committee report (NRC, 2008) emphasized the importance of Centaur reconnaissance, stating that: “Detailed study of these objects should greatly expand understanding of the history of volatiles in the solar system....(and these bodies) could prove to have sampled regions of the nebula and be rich in the types of organics not sampled on Earth or by previous missions To (study) these bodies ... close flybys are required.” Further supporting these earlier documents, the 2011 Planetary Decadal Survey (NRC, 2011) concluded that “Missions to Trojan or Centaur objects could provide information on their sources, as well as basic characterization and are important goals for the future”.

Therefore, we aim to visit these bodies for the first time, and characterize their geology, composition, comae, sources of activity, and ring/dust structures. Visiting Centaurs of different size classes will help us understand their origin and evolution, allow important comparisons to the KBOs visited by the *New Horizons* spacecraft (the Pluto-system and the 35-km-across Arrokoth), and provide a window into the transition of scattered-disk KBOs into comets.

1.2. A space telescope in the outer solar system

Even though Chiron is much closer to Earth than the Kuiper Belt, there is still significant cruise time in any spacecraft journey to Chiron. We plan to use this cruise for other science opportunities including both additional planetary science flybys (asteroids, comets, and/or other Centaurs) and astrophysical observations. A space telescope with one or more instruments will take advantage of the platform created by this mission, allowing it to fill critical scientific holes in the future space telescope fleet (see section 3.1).

Thus in addition to the planetary flyby instruments, this mission concept includes resources for one astrophysics cruise science telescope. A requirement for such instrumentation is that the science provided be unique and compelling, not duplicative with current or accepted missions on the nominal mission timescale. Zemcov et al. (2018) recently detailed several astrophysical investigations possible with the *New Horizons* flyby planetary instruments, taking advantage of its outer solar system location. Though the mission described here will not reach the large heliocentric distance of *New Horizons*, it will include instrumentation specifically designed to take advantage of the unique mission design, rather than simply rely on existing instruments designed for very different purposes. The expectation is that any such instrument will observe at wavelengths inaccessible or inefficient from the ground. In addition, the unusual, deep Solar System trajectory of this mission provides several exciting astrophysics possibilities, owing to the following attributes.

1.2.1. Low background

UV observations have significantly lower background for telescopes located outside of Earth orbit, i.e., away from the terrestrial airglow. Optical and near-IR observations also have lower zodiacal backgrounds at the heliocentric distances this mission will reach, and a cold telescope will lower the near-IR thermal background, even without implementing a full cryogenic design. Such low backgrounds are particularly enticing for studying the extragalactic background light (Cooray, 2016; Lauer et al., 2021), as well as the structure of the zodiacal cloud (e.g., Matsuura et al., 2017).

1.2.2. Atmosphere-free observations

Observing from space, free from the IR and UV absorption and emission of the Earth's atmosphere, provides access to wavelengths that are not easily accessed from the ground. Examples include UV observations bluewards of the atmospheric cutoff at 320 nm, as well as observations in the terrestrial IR water bands at 1.4 and 1.8 μm .

1.2.3. Unique vantage point

Far from Earth, this spacecraft could observe targets from a very different vantage point than Earth-orbiting and L2 facilities. As one example of such science, Laine et al. (2020) recently reported on *Spitzer Space Telescope* observations of the binary supermassive black hole system OJ 287 as the 150 million solar mass black hole secondary plunged through the accretion disk of the 20 billion solar mass black hole primary, producing luminous flares within 4 h of the predicted time. Such events only occur twice per 12 years, and the timing predictions rely on consideration of high-order relativistic effects. Because of the location of OJ 287 relative to the Sun, no terrestrial or Earth-orbiting telescopes could observe this event, but *Spitzer* could due to its Earth-trailing orbit. In addition, observing Galactic microlensing events far from Earth can help break degeneracies in the modeling, allowing better characterization of the lensing object mass and distance. Finally, early localization of gamma-ray bursts (GRBs) relied on relative timing of the short, high-energy flares from multiple NASA facilities. Though GRB science has moved beyond such crude localizations, similar triangulation might, in principle, be a useful and unique scientific capability for an astrophysics instrument on a space-born platform in the outer Solar System.

1.3. Overarching mission requirements

For development of the mission concept, we established a set of mission requirements and goals that would ensure we meet the above science and engineering objectives. Our requirements stem from the anticipated constraints of potential future flight and funding opportunities, as well as practical considerations of the desired performance and the desired low-risk posture. In order to perform the study, we needed to select some bounds to the parameter space, but many of these requirements stated below could be adjusted and still produce a viable mission.

1. Launch no later than December 31, 2029. Although later launch dates are also viable, we choose this as a practical upper bound for this study due to anticipated flight opportunities.
2. Complete all flybys and data return by December 31, 2039. This value yields an ~ 10 -year flight lifetime for the prime mission. Although 10 years is by no means a hard limit to spacecraft mission duration (many have performed longer), we chose this value as a baseline to achieve the science goals over a reasonable time horizon and also to minimize perceived risk.
3. Be solar powered and avoid the launch of radioactive materials for any purpose. We set this requirement due to the complexity and schedule risk of acquiring a nuclear launch license, along with the uncertainties in the future supply of plutonium (^{238}Pu) for use on spacecraft missions (Mosher, 2017).
4. Design the mission using existing technologies (thus requiring no new technology development).
5. Fly by 2060 Chiron and at least two other primitive bodies (for a total additional ΔV cost of $< 2 \text{ km s}^{-1}$ for the two additional objects), conducting flyby observations with a suite of planetary science instruments at each.
6. Conduct an intensive mission of astrophysics during interplanetary cruise. We set a goal of conducting astrophysical observations for 90% of every year in cruise.
7. Achieve a Chiron flyby velocity less than or equal to 7 km s^{-1} .
8. Achieve a Chiron flyby approach phase angle greater than 10° .
9. Encounter Chiron at a solar distance less than $\sim 12 \text{ AU}$ so as to enable the solar-powered mission. See section 3.3 for additional details.
10. The threshold payload shall consist of an IR mapping spectrometer, a high-resolution panchromatic imager, and an ultraviolet mapping spectrometer as the planetary science payload, and a 0.5-m class diameter astrophysics telescope to feed the astrophysical science.
11. The baseline payload shall also include 8–10 cubesats. We anticipate this number will be viable given the mass constraints but the specific number will be determined by the individual experiments of each cubesat.
12. Meet the payload resources/accommodation enveloped requirements (see Table 5).
13. Deliver a dry mass equal to or greater than $\sim 1500 \text{ kg}$ on a trajectory to fly by Chiron. This requirement stems from the dry mass of the NASA *Lucy* mission spacecraft. We modelled a broadly similar spacecraft but with modifications such as larger solar arrays, a larger communication system, and the addition of a solar electric propulsion (SEP) system (more details below).
14. Be viable on a launch vehicle with similar capability to the SpaceX Falcon Heavy.
15. Exclude a Jupiter gravity assist to avoid the need for radiation shielding.
16. Exclude a Venus gravity assist to simplify the thermal design.
17. Meet spacecraft and ground system redundancy standards appropriate to a NASA New Frontiers mission.
18. Fit within a $\$1.3\text{B}$ cost (FY25) for all activities and mission phases through Phase E end of mission (EOM). This cost includes 30%

reserves on phases A-D and 15% reserves on phases E and F (see section 4), but excludes tracking and data services, and the cost of 8–10 6U cubesats, which would be contributed by mission partners.

19. Meet NASA planetary protection requirements for its flyby targets and gravity assist flybys.

We used these requirements to design a trajectory, and then examined different possible mission architectures during a NASA Jet Propulsion Laboratory (JPL) Team-X session. The results of this study and the baseline mission concept that resulted are described below.

2. Mission design

2.1. Mission design description and procedure

For this analysis, we adopted the capabilities of the SpaceX Falcon Heavy Recoverable and Expendable as launch vehicle options. Given the above requirements to visit multiple small bodies and the need for flight times less than ~ 10 years, the ΔV involved in this mission is relatively large. Two options for propulsion systems were considered: (i) bipropellant (biprop) impulsive and (ii) low thrust engines powered by a SEP system. SEP was determined to be the best option because biprop would require a very large propellant mass due to the high necessary ΔV (typically greater than $4\text{--}5\text{ km s}^{-1}$ for the studied trajectories), which also could have large impacts on the spacecraft design. We instead adopted a SEP system capable of producing 60 KW of power at 1 AU.

Mission design was performed using the JPL in-house tools *Star* and *ZoSo*. *Star* is a patched-conic broad search tool and *ZoSo* is *Star*'s powerful optimizer. To begin, we used *Star* to performed a broad patched-conic search of all feasible trajectories that satisfy the mission constraints in an impulsive mode. Then *ZoSo* converts the converged trajectory into low thrust mode (SEP) and optimizes the trajectory again. There is always more than one optimized trajectory that meets the requirements; however, some are more compelling. For this mission, we started with the final target, Chiron, and allowed for Earth and Mars gravity assists. After optimizing this trajectory, we added more flyby targets using additional ΔV . The results of this process are described below.

2.2. Example trajectories

Here we present the initial trajectory results using chemical impulsive (biprop) and then the same trajectory is converted to the low thrust (SEP) propulsion systems that meets the mission requirements. Each example trajectory plot includes several kinds of information: i) dates for each major flight event (launch, flyby, etc.); ii) flyby velocity (V_∞); iii) launch declination angle (Dec.); iv) flyby altitude (Alt); v) flyby approach solar phase angle (Phase), which is the angle between the approaching spacecraft V_∞ and target heliocentric position vector; vi) the Sun-Earth-Probe angle (sep), vii) distance of the spacecraft from the Sun at each flyby (S); and viii) distance between the spacecraft and Earth at each flyby (E).

2.2.1. Bipropellant chemical impulsive propulsion system results

Figs. 3 and 4 show trajectories using a biprop impulsive propulsion system consisting of Nitrogen Tetroxide and Hydrazine as the oxidizer and the fuel, respectively, with an assumed specific impulse (I_{sp}) of 320 s. The first such trajectory (Fig. 3) has one Earth gravity assist (EGA) with a higher launch C_3 ($50\text{ km}^2\text{ s}^{-2}$), while the second one has a Mars gravity assist (MGA) followed by an EGA, and a much lower launch C_3 ($26.7\text{ km}^2\text{ s}^{-2}$). The first trajectory would require 2,382 kg of biprop mass and the second would require 5,968 kg. The second trajectory (Fig. 4) requires much more biprop mass because it has much lower launch C_3 . Preliminary analysis by our flight system design team indicated that these propellant loads would result in launch masses that would exceed the capability of even the higher performance Falcon Heavy (FH) Expendable launch vehicle. However, after conversion to SEP, this second trajectory worked well for our mission concept (see below).

2.2.2. Low thrust propulsion system results

We baseline one NASA Evolutionary Xenon Thruster (NEXT) ion engine (Hoskins et al., 2007) as the propulsion system (see section 3.3 and Table 2 for a description of the NEXT engine) and the Falcon Heavy Recoverable as our launch vehicle. Fig. 5 shows a SEP trajectory with two planetary gravity assists, first at Mars and then at Earth, and two planetary science flybys before arrival at Chiron. For promising trajectories, the JPL Horizons database of asteroids, comets, and Centaurs was

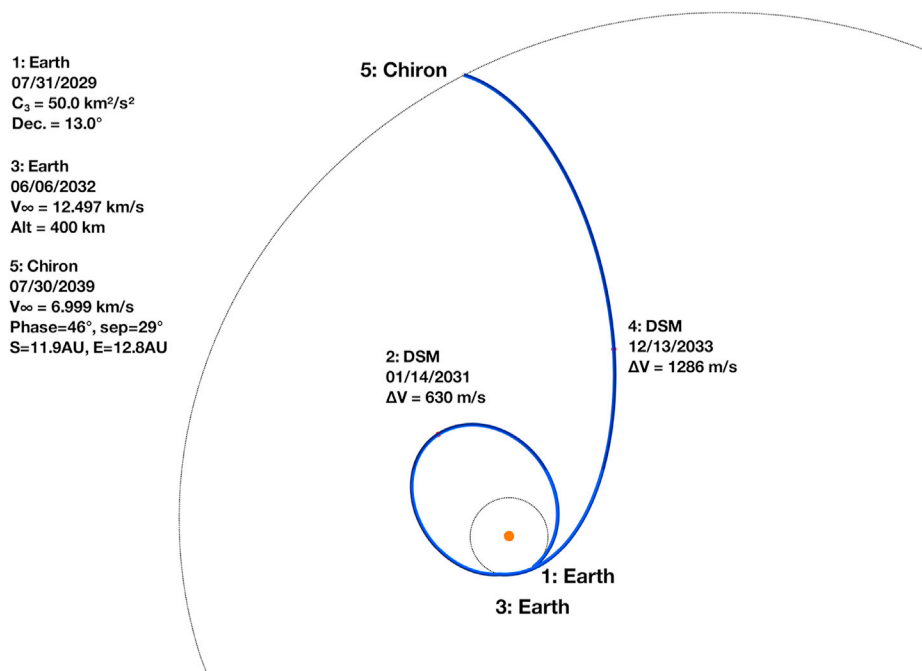


Fig. 3. Chemical biprop example design using a Falcon Heavy Expendable with one gravity assist (Earth). The dry mass delivered at Chiron is 2,866 kg and the biprop mass needed is 2,382 kg.

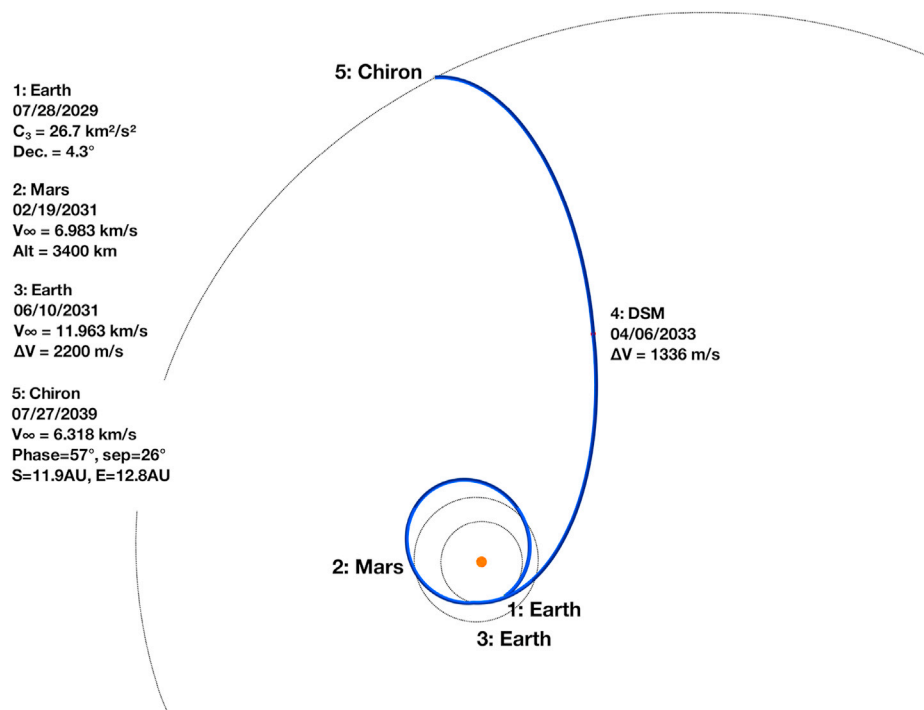


Fig. 4. Chemical impulsive example trajectory using a Falcon Heavy Expendable with two gravity assists (Mars then Earth). The dry mass delivered at Chiron is 2,904 kg and the biprop mass needed is 5,968 kg.

Table 1
Example SEP trajectory specifications (as shown in Fig. 5).

| Parameter | Value for Example Trajectory | Comparison to Stated Requirements |
|---|------------------------------|-----------------------------------|
| Launch date | 8/22/2029 | Exceeds |
| Arrival date | 8/22/2039 | Exceeds |
| MGA date | 3/16/2031 | N/A |
| EGA date | 6/9/2031 | N/A |
| Panopaea flyby | 12/16/2031 | N/A |
| 2017 GZ8 flyby | 12/9/2033 | N/A |
| Time-of-flight | 10 yr | N/A |
| Chiron V_∞ | 6.408 km s^{-1} | Exceeds |
| Chiron approach phase angle | 60° | Exceeds |
| Chiron distance from the Sun | 11.9 AU | Exceeds |
| Low thrust ΔV | 5.305 km s^{-1} | N/A |
| Delivered dry mass at Chiron | 2,314 kg | Exceeds |
| Xenon propellant | 337 kg | N/A |
| Launch C_3 ($\text{km}^2 \text{ s}^{-2}$) | 26.7 | N/A |
| Launch mass capability (kg) | 3,090 | N/A |
| Launch wet mass (kg) | 2,651 | N/A |
| Launch vehicle | Falcon Heavy (Recoverable) | Meets |
| Number of small bodies visited before Chiron | 2 | Meets |

Table 2
SEP system specifications.

| Item | Specification |
|--|------------------------------|
| Solar array | $\geq 60 \text{ kW}$ at 1 AU |
| Engine | 1 NEXT Ion Engine |
| Max input power (nominal) | 7.2 kW |
| Max power used in trajectory | 7.14 kW |
| Max I_{sp} (nominal) | 4,195 s |
| Max I_{sp} used in trajectory | 4,142 s |
| Equivalent I_{sp} used in trajectory | 3,984 s |
| Max thrust used in trajectory | 200 mN |
| Max Xenon mass (with margin) | 485 kg |

searched to find flyby candidates that could be visited within an allowance of additional propellant above that required to reach Chiron of $1 \text{ km s}^{-1} \Delta V$ or less. Multiple interesting targets were found on any of the sample trajectories, some for as little as tens to hundreds of m s^{-1} of additional ΔV . For the example SEP trajectory shown in Fig. 5, we included 2017 GZ8, which is a smaller Centaur ($\sim 5 \text{ km}$ across assuming an albedo of 0.15 similar to other small KBOs) and 70 Panopaea, which is a large main belt asteroid with a mean diameter of $\sim 120 \text{ km}$ (Tedesco et al., 2004). Both objects are primitive bodies that would reveal key information about planetary formation. For the trajectory shown in Fig. 5, the baseline ΔV was 4.007 km s^{-1} and the additional ΔV required to reach these two objects brought the total ΔV to 4.288 km s^{-1} . Table 1 presents some of the specifications of the trajectory shown in Fig. 5.

Apart from the significant savings in propellant (and hence spacecraft) mass, another advantage of the SEP system is that ΔV used for additional target flybys can be obtained with only a small added mass of Xenon with respect to the mass of the spacecraft. For example, adding 1 km s^{-1} of ΔV expenditure ($5.305 \text{ km s}^{-1} + 1.0 \text{ km s}^{-1} = 6.305 \text{ km s}^{-1}$) costs only 58.5 kg of Xenon, making the total Xenon mass 395.1 kg. In this case, the mass delivered to Chiron is $\sim 2,256 \text{ kg}$. Filling the Xenon tank to its full capacity of 485 kg would allow the mission to take advantage of the full performance of the Falcon Heavy Recoverable and support a delivered mass of up to $\sim 2600 \text{ kg}$, providing significant additional margin against mass growth and/or significant flexibility in targeting additional flybys. For these reasons, and the fact that the large solar array needed for Chiron operations can provide ample power for a significant part of the trajectory, SEP emerged as the favored propulsion option. Table 2 summarizes the SEP system specifications.

Fig. 6 shows the NEXT ion engine coast and SEP thrust plan for the trajectory in Fig. 5, and Table 3 presents the coast and SEP thrust durations throughout the mission. We used an 85% engine duty cycle. In this example, the engine is off (i.e., coasting) when performing the Mars gravity assist (Mar 16, 2031), but the engine is thrusting when performing the EGA (Jun 9, 2031). This trajectory can be adjusted by adding short forced coast periods, which is where the trajectory is designed such that the engine can be turned off at specified times for several weeks

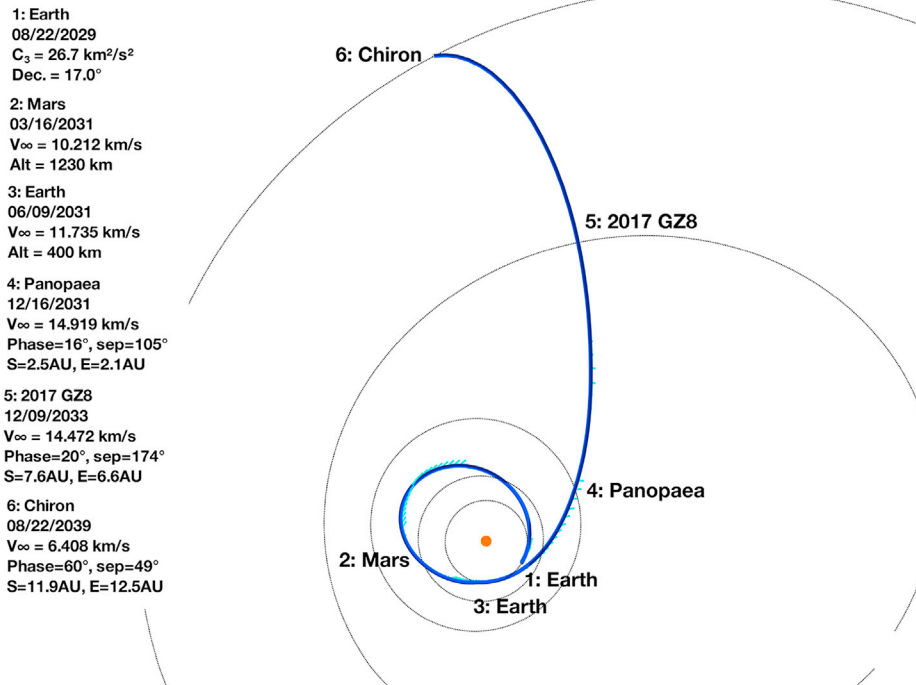


Fig. 5. Example SEP trajectory using a Falcon Heavy Recoverable with two gravity assists (Mars then Earth). This trajectory includes with two Centaur flybys (2017 GZ8 and Chiron) and one main belt asteroid flyby (Panopaea). The small light blue bars extending off of the trajectory show the timing and magnitude of SEP thrusting (also see Fig. 6). The dry mass delivered at Chiron is 2,314 kg for the full capability of the launch vehicle and the Xenon mass needed is 336 kg.

before and/or after spacecraft events that require specific pointing (for example it will be turned off during the planetary flybys, or could be designed to be turned off during EGA if pointing is required for downlink, etc.). In these cases, the mission design program would be able to compensate for the engine being off during forced coast periods by adjusting the thrust magnitude and duration at other times in the mission.

3. Mission implementation

This section describes a baseline description of the mission's key hardware components, including the primary science instruments (section 3.1), the cubesats (section 3.2), and the spacecraft (section 3.3).

3.1. Science payload

The primary science payload includes a set of instruments designed to provide a comprehensive remote sensing investigation of the planetary flyby targets, as well as an astrophysics telescope to provide science during the long travel times between flyby targets. We describe each in turn.

3.1.1. Planetary flyby instruments

We baseline a complement of three remote-sensing instruments that meet our desired science goals and will perform a broad science investigation of Centaurs. The three instruments envisioned are: (1) a visible imager and IR spectral mapper similar to the L/Ralph package (a combination of two instruments, a color camera and a high spectral resolution imaging spectrometer) developed for the NASA *Lucy* mission (Olkin et al., 2021), which itself has high heritage from the Ralph instrument flown on *New Horizons* (Reuter et al., 2008); (2) a high-resolution visible imager, similar to the L'LORRI instrument developed for *Lucy* (Olkin et al., 2021), which itself has high heritage from the LORRI instrument flown on *New Horizons* (Cheng et al., 2008); and (3) a UV spectrograph, based on the Alice instrument on *New Horizons* (Stern et al., 2008) and

the Lyman Alpha Mapping Project (LAMP) on NASA's *Lunar Reconnaissance Orbiter* (LRO) mission (Gladstone et al., 2009). All three of these instruments are low-risk, high-TRL designs with significant flight heritage from multiple builds on previous successful flight missions. Table 4 provides key parameters for this baseline suite of instruments for the flyby planetary science observations based on the notional instruments mentioned above.

In addition, the spacecraft radio subsystem will be used to determine (or constrain) the masses of the larger flyby targets by measuring Doppler frequency shifts in the radio carrier caused by target gravitational forces perturbing the spacecraft motion. This radio Doppler method has a long history of measuring the masses of small Solar System bodies (e.g., Christensen et al., 1977; Pätzold et al., 2019). Combined with a volume estimate from imaging, the mass determination can allow an estimate of the planetary targets' bulk densities. Each target and trajectory geometry must be reviewed after the final selection to determine the precision to which masses and densities can be calculated. This implementation is based off of the *Lucy* mission where the densities of their Trojan asteroid targets will be constrained (Olkin et al., 2021). The *Lucy* mission utilizes an X-band telecommunication system and Doppler tracking of the spacecraft for 7 h on both approach and departure, starting at ± 2 hr out from closest approach.

3.1.2. Visible imager and IR spectral mapper

This type of instrument is designed to determine the colors and composition of flyby targets, perform panchromatic medium focal length imaging, and map extended ring/dust structures. The design used here is based on the L/Ralph instrument on *Lucy*, which has two primary components: the Multi-spectral Visible Imaging Camera (MVIC) visible/NIR imager, and the Linear Etalon Imaging Spectral Array (LEISA) IR spectral mapper. The imaging camera will be used for characterizing flyby target surface geology and for mapping craters, tectonic structures, and sites of past or present activity on Centaurs. Images from this instrument will also be used to define flyby target shapes and volumes. When combined with the radio Doppler mass measurements, shape and volume allow an

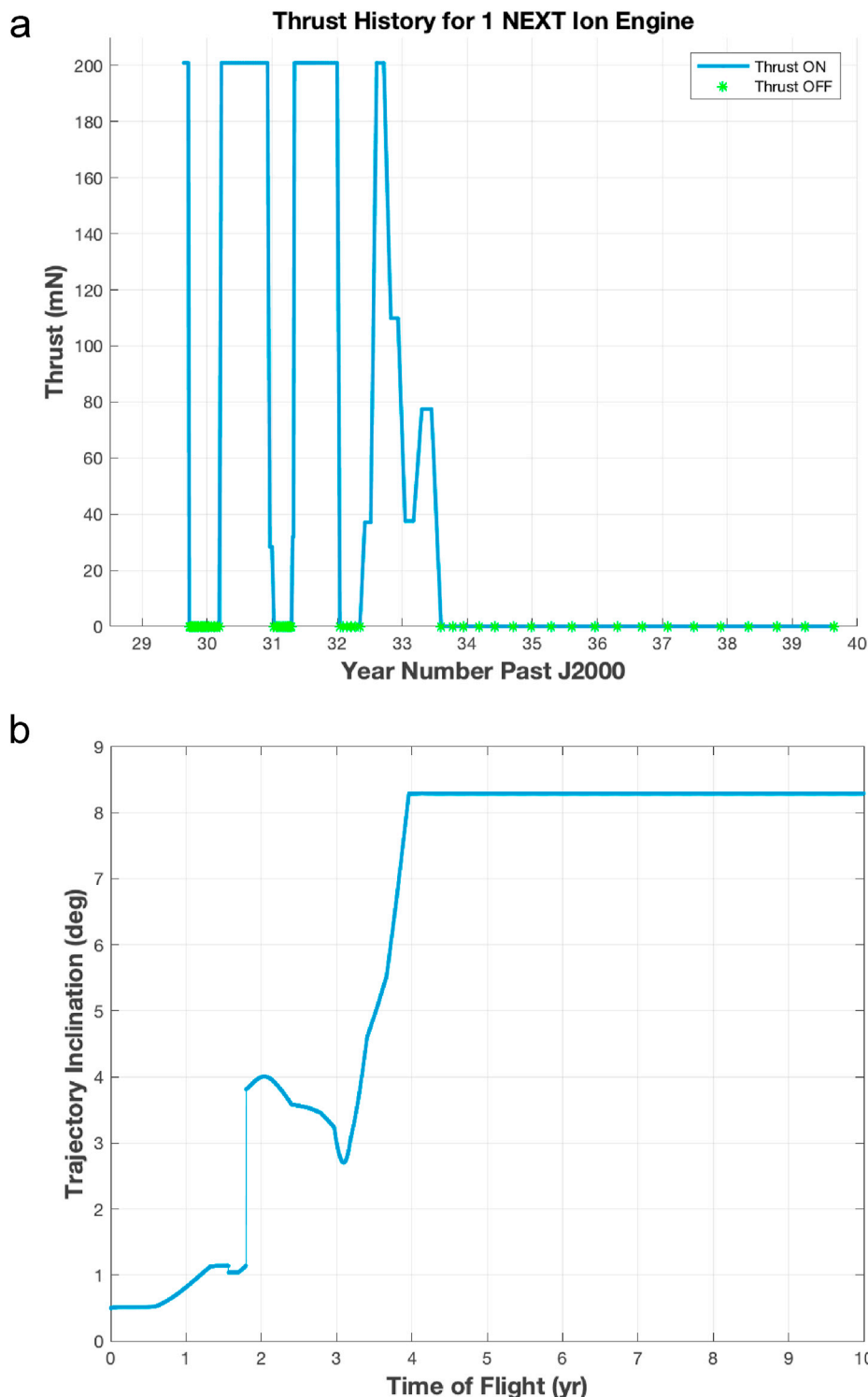


Fig. 6. (a) NEXT ion engine thrust and coast history and (b) spacecraft instantaneous inclination for the trajectory shown in Fig. 5.

estimate of target density, which provides important clues towards the internal structure of flyby targets. In addition, a color imager similar to MVIC can map the extended ring/dust structures of Centaurs such as Chiron, and search for surface and coma features indicative of current or past activity (e.g., plumes, sources of jets, or other coma particulates). An IR spectral mapper similar to LEISA will map the surface photometric composition, thereby measuring the distribution of compositional units, including target minerals, ices, salts, and organics.

3.1.3. High-resolution visible imager

The design used here is based on the *Lucy* L'LORRI long focal length imager (Olkin et al., 2021), which uses a 20.8 cm, f/12.6 Ritchey-Chrétien telescope with a 3-lens field flattener feeding a heavily baffled focal plane with a broadband (350–850 nm) optical filter and a high quantum efficiency 1024 × 1024 CCD detector. This type of instrument provides higher resolution imaging, reaching tens of meter scales, and operates in a single, broad optical band in order to maximize the signal-to-noise ratio. Science that will be enabled by this imager

Table 3
NEXT ion engine thrust/coast durations for the trajectory shown in Figs. 5 and 6.

| Engine Mode | Start | Stop | Duration |
|-------------|--------------|--------------|-----------|
| Thrust | Aug 22, 2029 | Sep 21, 2029 | 1 mo |
| Coast | Sep 21, 2029 | Mar 9, 2030 | 6 mo 19 d |
| Thrust | Mar 9, 2030 | Jan 11, 2031 | 10 mo 8 d |
| Coast | Jan 11, 2031 | Apr 18, 2031 | 3 mo 7 d |
| Thrust | Apr 18, 2031 | Jan 16, 2032 | 9 mo 3 d |
| Coast | Jan 16, 2032 | May 7, 2032 | 3 mo 22 d |
| Thrust | May 7, 2032 | Aug 6, 2033 | 1 yr 3 mo |
| Coast | Aug 6, 2033 | Aug 22, 2039 | 6 yr 16 d |

Table 4
Specifications for baseline flyby planetary instruments.

| | Visible/near-IR imager and near-IR spectral mapper | High-resolution optical imager | UV imaging spectrograph |
|----------------------------------|--|---------------------------------|------------------------------------|
| Recent Heritage Instrument | <i>Lucy/L'Orph</i> ^a | <i>Lucy/L'ORRI</i> ^a | <i>LRO/Alice LAMP</i> ^b |
| Spectral range, nm | 375–3800 | 450–850 | 60–200 |
| Mass, kg | 37 | 14 | 5 |
| Power, W | 30 | 12.4 | 5 |
| Est. Dimensions, cm ³ | 110 × 100 × 60 | 270 × 21 × 21 | 50 × 16 × 12 |
| Data rate, Mbit s ⁻¹ | 2 | 12.7 | 1 |

^a Olkin et al. (2021).

^b Gladstone et al. (2009).

Table 5
Flight system requirements.

| Item | Requirement |
|---|-----------------------------------|
| System | |
| Total flight system mass (dry/wet) | 1892/2651 kg |
| Radiation TID | <20 krad (RDM = 2) |
| Design lifetime | 130 mo |
| Payload | |
| Payload mass ^a | 337 kg |
| Payload power | 140 W |
| Payload max data rate | 12.7 Mbps |
| ACS | |
| Pointing control ^b | 1.8 arcsec |
| Pointing knowledge ^b | 3 arcsec |
| Pointing stability ^b | 3.6 arcsec/200 s |
| Slew ability | 0.015 rad s ⁻¹ |
| Stabilization type | 3 - axis |
| CDS | |
| Max. payload data rate | 30 Mbps |
| Data storage volume | 768 Gb |
| Telecom | |
| Band(s) | X, Ka |
| Antenna type, size, & number, gimbaled? | 3m HGA, gimbaled |
| Uplink rate | 2 kbps |
| Downlink rate | 2 Mbps (1 AU) to ~30 kbps (10 AU) |
| Power | |
| Articulated solar array? (Yes/No) | Yes |
| Propulsion | |
| No. of propulsion systems | 2 |
| Type(s) of system(s) | SEP/Hydrazine monoprop |
| Total SEP ΔV | 6300 m s ⁻¹ |
| Total monoprop ΔV^c | 180 m s ⁻¹ |

^a Includes all instruments, 10 cubesats (~8 kg each) and deployer

^b Based on notional astronomical instrument.

^c Assumes four targeted flybys at 20 m s⁻¹ each and 100 m s⁻¹ for TCMs.

ranges from characterizing the geology and geophysics of the flyby targets, to identifying small craters, to studying the extended ring/dust structure of Chiron, to identifying satellites of each flyby target. This camera will also be used for optical navigation to refine the flyby trajectories and identify potential hazards around the flyby targets.

3.1.4. UV spectrograph

This instrument will measure the composition and density of the Chiron coma in order to probe the source and rate of coma activity, including the production rates of parent molecular species resulting from sublimation. The design used here would be the seventh in a series of combined EUV/FUV Alice spectrographs for planetary missions designed, fabricated, and operated by SwRI. Previous iterations have flown on *New Horizons*, *Rosetta*, *LRO*, and *Juno*. This design is a slightly simplified/light-weighted modification of LAMP on *LRO* (Stern et al., 2009), which launched in 2009 and is fully operating today. For this version, some unnecessary *LRO*-specific items (e.g., a lunar terminator sensor and solar occultation port) will be removed.

3.1.5. Candidate cruise astrophysics instruments

The baseline plan includes a telescope comparable in scale to a NASA Small Explorer mission. We baseline a mass of 50 kg, requiring 15 W of power, and requiring a volume of $\sim 100 \times 100 \times 50$ cm³, which are values typical of Small Explorer-class missions. The expected aperture diameter is 0.5–0.8 m. The need for such astrophysical telescope assets is evidenced by the regular, high oversubscription to NASA calls for missions at this scale. As described above, both UV and IR options were considered for this study, but a formal selection will be made at a more advanced stage of mission development.

3.2. Cubesat ride along payloads

The mission will carry 8–10 6U cubesats. They will be released from two dispensers that will house five cubesats each. The objective of the cubesats is to further provide opportunities for taking advantage of mission design to accomplish additional science that the main spacecraft does not. There are many science possibilities for potential cubesat providers to take advantage of. We plan for the cubesat experiments to be contributed by universities, institutions, or nations. One scenario is for cubesats to be deployed from the mothership several days before a planetary flyby. The cubesats can then fly ahead or behind of the mothership, to flyby the opposite side of the body from the mother ship to provide high resolution “far side” imaging, usually not feasible on flybys. Chiron has a 5.9 hr rotation period (Bus et al., 1989; Luu and Jewitt, 1990; Marcialis and Buratti, 1993). 6U spacecraft are able to provide up to 200 m s⁻¹ ΔV for temporal separation of arrival times at flyby targets. In order to view the opposite side of Chiron in sunlight, a cubesat would need to arrive ~3 h before or after the mothership. For the trajectory shown in Fig. 5, and for arrival after the mothership, the cubesat would need to be launched 3.8 days ahead of the mothership's closest approach time (using the maximum of 200 m s⁻¹ additional ΔV).

Cubesats could alternatively be equipped with non-imaging instruments, such as magnetometer or a particle detector, that the mothership will not carry. Cubesats can also provide cruise science opportunities in astrophysics and heliophysics. This armada of cubesats will provide another important dimension of creativity and partnership to this mission's already diverse planetary and astrophysical science.

The volume of each cubesat dispenser will be approximately 70 cm × 33 cm × 47 cm. The mass of the two dispensers is approximately 70 kg total, in addition to an estimated mass of 10 6U cubesats at ~78 kg. There are no pyrotechnics in the dispenser. The release door will be operated by a DC brushless motor. Thermal control will keep the cubesats within –25 C to +45 C. The continuous heater power needed is 7W total. The cubesats will likely operate on battery power only, although some may use solar cells depending on the investigation. We estimate that a 6U cubesat would require approximately 120 W for science instruments, 240 W to downlink of the data to the mothership in 6 h via ultra-high frequency (UHF), <100W to operate avionics, plus thermal power for temperature management during a few-day long mission. In our baseline scenario, up to two cubesats could communicate with the mothership via a UHF link at one time.

3.3. Flight system concept

While it is still early in the development of this mission concept and no specific flight system has yet been selected, it is possible to sketch out the characteristics of the main spacecraft based on the science, instrument accommodation, and mission design details discussed above. The baselined concept is a single medium-to large-class flight system capable of hosting the payloads described above and also ensuring their ability to acquire and return data throughout the mission.

Perhaps the most defining trade was that between using conventional biprop chemical propulsion vs. SEP to accommodate the high ΔV demands of the preferred trajectory. As described in section 2 above, this trade was decided when it became evident that the high fuel mass required for the chemical-only trajectories would render the mission infeasible. Thus, the flight system concept developed for the mission is assumed to be based on a conventional SEP bus design with specific modifications to adapt to the unique mission requirements. The large solar arrays needed to support spacecraft power requirements at the Chiron encounter further strengthen the choice of SEP as they will provide sufficient power to operate the propulsion system through a large portion of the trajectory.

The selected electric propulsion system has two gimballed NEXT ion engines (Fig. 7), only one of which will be used at any given time, with the second carried for redundancy. NEXT engines, a recent development by NASA, are capable of operating at power ranges from 500 W to ~ 7 kW with a maximum specific impulse (Isp) of over 4000 s (<https://www1.grc.nasa.gov/space/sep/gridded-ion-thrusters-next-c/>). Xe propellant margin was added by sizing the Xenon load to allow provision of the ~ 6300 m s⁻¹ that would be required to achieve the maximum possible launch mass afforded by the launch vehicle (3090 kg launch vehicle capability for C₃ of 26.7 km² s⁻²).

In addition to SEP, the propulsion subsystem also incorporates a monopropellant hydrazine system to accommodate the need for discrete trajectory correction maneuvers (TCMs) around each flyby and a reaction control subsystem (RCS) for attitude maneuvers. We baseline four 5N thrusters for TCMs and eight 1N thrusters for the RCS. It is estimated that the TCMs necessary to execute the baseline trajectory will require a total of about 100 m s⁻¹ of ΔV capability over the course of the mission, with an additional 20 m s⁻¹ required for targeting and cleanup maneuvers for each flyby, resulting in a total hydrazine propellant mass (including RCS) of ~ 128 kg of hydrazine.

Power for the flight system will be provided by two large solar arrays. Given the large array size needed to generate adequate power at the maximum solar range of 12 AU during and after Chiron flyby, we adopted the use of MegaFlex arrays using IMM4 solar cells optimized for the low

intensity, low temperature (LILT) conditions experienced at this remote distance. Recent work at JPL has tested these cells for performance under LILT conditions equivalent to those encountered at ranges as distant as Uranus (at 20 AU) with good results (Boca and MacFarland, 2020).

The power requirements for the spacecraft at Chiron are estimated at ~ 500 W to allow operation of the spacecraft and its three planetary instruments (the astrophysics payload will be powered off during planetary flybys). This power estimate is based on comparable SEP bus designs. The resulting array design requires two wings, each ~ 12 m diameter. This is in-family with, although somewhat larger than, the 10 m diameter solar array test article developed for NASA's SEP technology development program (Fig. 8) and well within the range that is considered a "low-risk" increment for this array design (Murphy et al., 2016).

Design drivers on the electrical power subsystem include supporting a 100 V power bus for the SEP system, while providing a 30 V power bus for the rest of the spacecraft. Design of the power subsystem will be similar to other SEP designs; in this case, initial design concepts draw on the design of *Psyche*, a joint JPL/Maxar SEP flight system currently in late stages of development, for which launch is planned for August 2022.

The telecommunications subsystem design is driven by the need to return all data from the flybys, from the cubesats, and from the astrophysics payload in a timely manner, culminating with the flyby of Chiron at a maximum Earth range of up to 12 AU. The communications system also supports an UHF relay capability to provide a link with the cubesat payloads.

Initial estimates of downlink data volume requirements are ≤ 1 Tb per year for the astrophysics (consistent with an Explorer-class instrument) and about 32 Gb per small body flyby. This data volume during the later years of the mission, when the spacecraft is farther from the Sun, is a major driver that will require a balance of data return strategy (e.g., taking advantage of times the spacecraft is not making observations) and telecom subsystem design. A baseline design requirement has been adopted to provide a system capable of > 1 Mbps from close ranges of 1–2 AU, and at least 15 kbps from a range of 10 AU (this Saturn-like range was used for scaling purposes although it is recognized that the final Chiron encounter is at ~ 12 AU).

Fig. 9 shows telecom trades considered, indicating the significant improvements that could be obtained with moderate changes to HGA size and/or TWTA radio frequency (RF) power. To satisfy the requirements just stated, we baselined a Ka band telecom subsystem with redundant 25 W traveling wave tube amplifiers (TWTAs) communicating through a steerable 3-m high gain antenna (HGA). This actually provides about 30 kbps data return from 10 AU to > 2 Mbps from an Earth distance of 1 AU (all link calculations assume rates to a 34 m NASA Deep Space Network (DSN) station, with 3 dB of margin).

Requirements on the command and data handling (C&DH) subsystem include providing command and control for all spacecraft subsystems, as well as interfaces for the astrophysics and planetary instruments, sensor

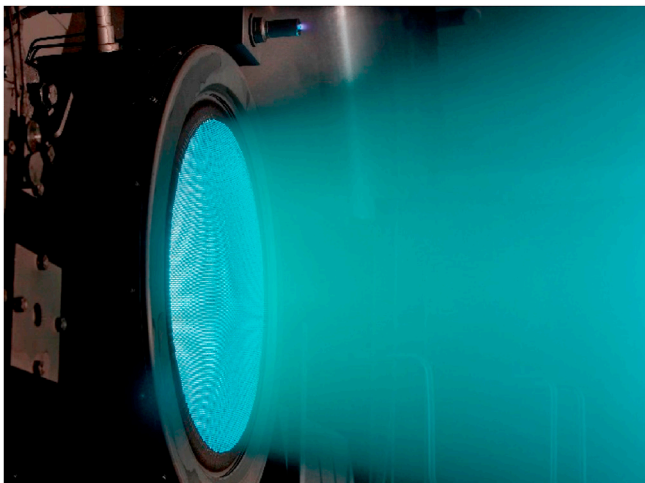


Fig. 7. NEXT ion thruster in test chamber. Image credit: NASA.

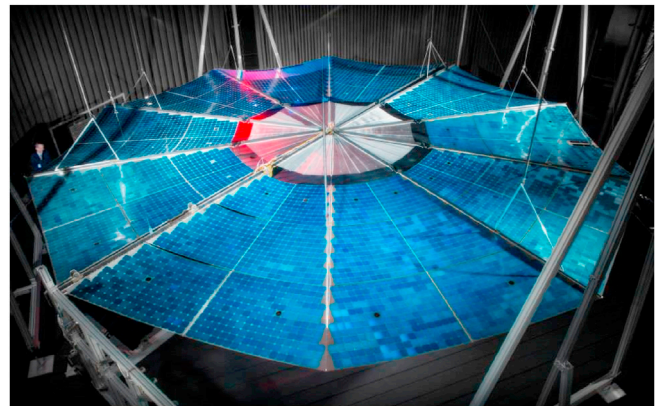


Fig. 8. MegaFlex 10 m array in deployment testing.

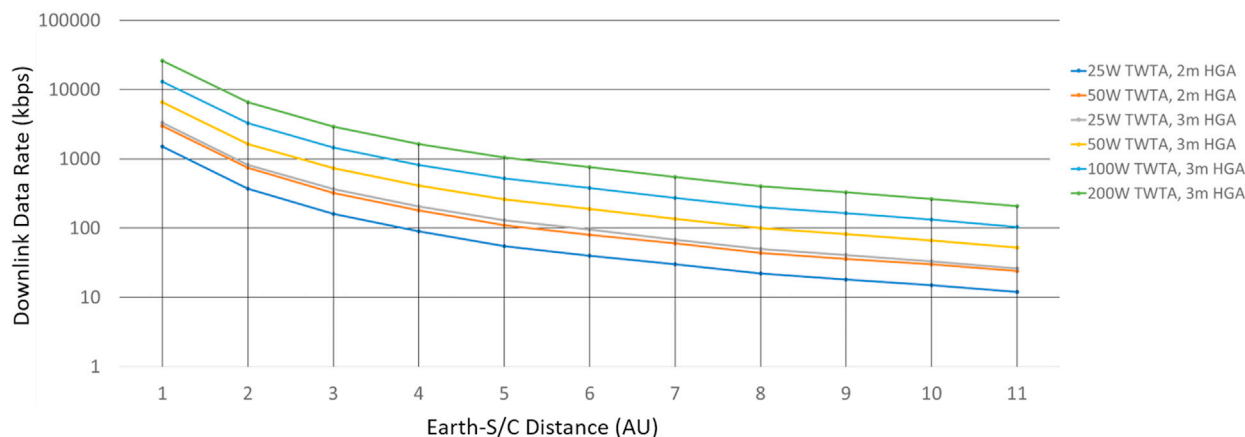


Fig. 9. Downlink data rate at Ka band to a 34m DSN station vs. Earth-spacecraft distance.

interfaces for guidance, navigation, and control (GNC) sensors and motor control for actuators and mechanisms. The C&DH subsystem is internally redundant to eliminate the possibility of single point failures.

The attitude control subsystem (ACS) is required to provide the pointing accuracy, stability, and knowledge necessary to make the required planetary and astrophysical observations. ACS sensors include redundant star trackers, inertial measurement units, and Sun sensors. Attitude is maintained and controlled using reaction wheels, with momentum unloading provided by the RCS thrusters. Fast slews required during flyby operations are facilitated by mounting the planetary instruments on a two-axis instrument scan platform (Fig. 10). Redundant terminal tracking cameras are mounted on the scan platform to facilitate tracking during flybys. A second scan platform is provided for the astrophysics payload to allow unrestricted pointing (independent of thrust vector) and also the pointing of the planetary payloads) during periods of SEP thrusting in cruise.

The flight system assumes a conventional structural design that provides support for the payload instruments on scan platforms and cubesats in their deployers, as well as two single-axis gimballed solar arrays and a gimballed 3-m HGA. The structure was sized to support launch loads assuming the fully margined wet spacecraft mass.

The spacecraft employs a thermal control system able to accommodate environmental conditions from 1 AU to >12 AU while keeping all instrument and flight system elements within their allowable flight temperatures. Radiators with embedded heat pipes are used to reject heat from the SEP system when in operation. For the remainder of the bus, the thermal control system utilizes radiators, louvers, blankets, and heaters to maintain spacecraft components within temperature limits. Radiators are sized to maintain all units within allowable flight temperatures for the worst-case hot environmental and operational configuration. For distant operations, heat loss is minimized by blanketing the spacecraft in multi-layer insulation (MLI). Radiator area is reduced by strategically distributing the powered components throughout the spacecraft bus to efficiently utilize waste heat and reduce system heater power requirements. Redundant cross-strapped heaters and temperature sensors are used with mechanical or software-controlled thermostats distributed throughout the spacecraft to monitor thermal health and maximize operational flexibility during the mission.

A summary of notional requirements for the flight system is shown in Table 5.

4. Cost

Flight system development costs were estimated by JPL's Team X using three approaches: historical data for missions of similar type (in this case mostly New Frontiers), rules of thumb based on costs of subsystems for similar master equipment list (MEL) and power equipment

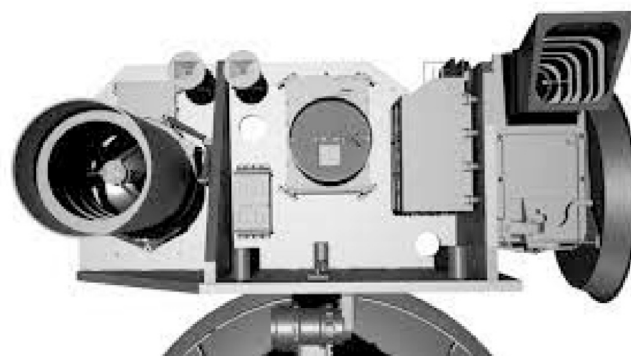


Fig. 10. Planetary instrument pointing platform (*Lucy* IPP shown as example). The platform is ~125 cm across.

list (PEL), and direct mission cost comparison. Independent parametric model estimates were also generated as a crosscheck. The cost estimate is given in Table 6. It was assumed that the spacecraft is a modified communication satellite purchased from one of the well-established primes in this arena. Instrumentation costs are analogs from historically similar instruments, including the costs to develop the astrophysics payloads hosted on the spacecraft. Ground segment and operations costs were estimated with a model based on past JPL missions. Launch costs were taken from publicly available statements from SpaceX. Note that costs were included for launch services, DSN antenna usage, standing review boards, education and public outreach, and launch insurance.

5. Conclusion

We have studied a New Frontiers class planetary science mission that has the innovative aspect of doing significant astrophysics during its many years of interplanetary cruise. We developed a working and technically feasible mission concept at approximately the level of a pre-phase A NASA mission study through multiple workshops and focused trade studies. The mission's primary planetary science targets are the as yet unexplored Centaurs. Centaurs are scientifically valuable, escaped bodies from the Kuiper Belt that orbit largely within the realm of the giant planets, where they are more accessible than KBOs themselves. The largest of the multiple Centaurs to be reconnoitered with this mission is 2060 Chiron, a 220 km diameter body with known atmospheric activity and rings. The mission can be accomplished with a launch on a Falcon Heavy Recoverable in the late 2020s and culminates with a flyby of Chiron by 2039, and can rely entirely on solar power using 12-m-diameter MegaFlex arrays. In space electric propulsion was selected over a large chemical biprop system; the implemented SEP system is based

Table 6
Cost estimate.

| Element name | Cost estimate (FY20 \$M) |
|--|--------------------------|
| Phases A-D | |
| Management | 37.7 |
| System engineering | 22.0 |
| Safety and mission assurance | 10.7 |
| Science team | 23.7 |
| Payload | 133.4 |
| Spacecraft | 289.0 |
| Mission operations services (MOS) | 14.2 |
| Falcon Heavy launch vehicle | 115.0 |
| Ground-data systems (GDS) | 13.4 |
| Assembly test and launch operations (ATLO) | 39.7 |
| Reserves on phases A-D (30%) | 199.2 |
| Phase E/F (includes 15% reserves) | 266.3 |
| Additional logistics and mission expenses | 95.0 |
| Total | 1,259.3 |

around redundant NEXT thrusters. The mission payload consists of a comprehensive, heritage-based planetary science remote sensing payload, a 0.5-m-class astrophysics telescope for UV or IR studies with down-select planned at a later stage of mission definition, and ten 6U cubesats. Communications are provided through a 3m diameter HGA at both X and Ka band. The mission cost is estimated to be \$1,259M, including reserves, launch, and mission operations.

Author statement

Kelsi N. Singer: Conceptualization, Validation, Formal analysis, Investigation, Writing - Original Draft, Writing - Review & Editing, Visualization. **S. Alan Stern:** Conceptualization, Validation, Investigation, Writing - Original Draft, Writing - Review & Editing, Project administration, Funding acquisition. **John Elliott:** Conceptualization, Methodology, Validation, Formal analysis, Writing - Original Draft, Writing - Review & Editing, Visualization. **Reza R. Karimi:** Methodology, Software, Formal analysis, Writing - Original Draft, Visualization. **Daniel Stern:** Conceptualization, Investigation, Writing - Original Draft, Writing - Review & Editing. **Arthur B. Chimelewski:** Conceptualization, Validation, Writing - Original Draft, Writing - Review & Editing, Project administration, Funding acquisition. **Michael J. Fong:** Formal analysis, Writing - Review & Editing. **John Andrews:** Validation, Writing - Original Draft, Project administration. **William F. Bottke:** Conceptualization, Writing - Review & Editing. **Catherine B. Olkin:** Conceptualization, Writing - Review & Editing. **Paul Propster:** Writing - Review & Editing, Project administration. **Sam W. Thurman:** Writing - Review & Editing, Project administration.

Declaration of competing interest

The authors declare that they have no known competing financial interests or personal relationships that could have appeared to influence the work reported in this paper.

Acknowledgments

KNS, SAS, WFB, JA, and, CBO thank Southwest Research Institute for IRAD funding to carry out this mission concept study. The work of JE, RRR, DS, ABC, MJF, PP, and SWT was carried out and supported by the Jet Propulsion Laboratory, California Institute of Technology. The authors thank Mr. Adam Hamilton, Mr. Walt Downing, and Dr. James Burch of SwRI and Dr. Robert Braun of the Jet Propulsion Laboratory for their support leading to this project.

Appendix A. Supplementary data

Supplementary data to this article can be found online at <https://doi.org/10.1016/j.pss.2021.105290>.

References

- Boca, A., MacFarland, C., 2020. Towards a photovoltaic power source for missions to Uranus. In: *Advanced Power Systems for Deep Space Exploration* (abstract).
- Braga-Ribas, F., et al., 2014. A ring system detected around the Centaur (10199) Chariklo. *Nature* 508, 72.
- Bus, S.J., Bowell, E., Harris, A.W., Hewitt, A.V., 1989. 2060 Chiron: CCD and electronographic photometry. *Icarus* 77, 223. [https://doi.org/10.1016/0019-1035\(89\)90087-0](https://doi.org/10.1016/0019-1035(89)90087-0).
- Bus, S.J., Bowell, E., Stern, S.A., A'Hearn, M.F., 1991. Chiron: evidence for historic cometary activity. *Asteroids, Comets, Meteors* 765, 34 (abstract).
- Bus, S.J., et al., 1996. Stellar occultation by 2060 Chiron. *Icarus* 123, 478–490. <https://doi.org/10.1006/icar.1996.0173>.
- Cheng, A.F., et al., 2008. Long-range reconnaissance imager on new horizons. *Space Sci. Rev.* 140, 189–215.
- Christensen, E.J., Born, G.H., Hildebrand, C.E., Williams, B.G., 1977. The mass of Phobos from Viking flybys. *Geophys. Res. Lett.* 4, 555. <https://doi.org/10.1029/GL004i012p00555>.
- Cooray, A., 2016. Extragalactic background light measurements and applications. *Roy. Soc. Open Sci.* 3, 150555. <https://doi.org/10.1098/rsos.150555>.
- Crovisier, J., et al., 1995. Carbon monoxide outgassing from comet p.solarschwassmann-wachmann 1. *Icarus* 115, 213. <https://doi.org/10.1006/icar.1995.1091>.
- Drahus, M., Yang, B., Lis, D.C., Jewitt, D., 2017. New limits to CO outgassing in Centaurs. *Mon. Not. Roy. Astron. Soc.* 468, 2897. <https://doi.org/10.1093/mnras/stw2227>.
- Duncan, M.J., Levison, H.F., 1997. A scattered comet disk and the origin of Jupiter family comets. *Science* 276, 1670. <https://doi.org/10.1126/science.276.5319.1670>.
- Elliot, J.L., et al., 1995. Jet-like features near the nucleus of Chiron. *Nature* 373, 46–49. <https://doi.org/10.1038/373046a0>.
- Enzian, A., Cabot, H., Klinger, J., 1997. A 2 1/2 D thermodynamic model of cometary nuclei. I. Application to the activity of comet 29P/Schwassmann-Wachmann 1. *Astron. Astrophys.* 319, 995.
- Fernández, J.A., Helal, M., Gallardo, T., 2018. Dynamical evolution and end states of active and inactive Centaurs. *Planet. Space Sci.* 158, 6–15. <https://doi.org/10.1016/j.pss.2018.05.013>.
- Fornasier, S., et al., 2013. TNOs are cool: a survey of the trans-neptunian region. VIII. Combined Herschel PACS and SPIRE observations of nine bright targets at 70–500 μ m. *Astron. Astrophys.* 555, A15. <https://doi.org/10.1051/0004-6361/201321329>.
- Gladman, B., Kavelaars, J.J., Petit, J.-M., Morbidelli, A., Holman, M.J., Lored, T., 2001. The structure of the Kuiper belt: size distribution and radial extent. *Astron. J.* 122, 1051–1066. <https://doi.org/10.1086/322080>.
- Gladstone, G.R., et al., 2009. LAMP: the Lyman Alpha mapping project on NASA's lunar reconnaissance orbiter mission. *Space Sci. Rev.* 150, 161–181. <https://doi.org/10.1007/s11214-009-9578-6>.
- Gomes, R.S., Fernández, J.A., Gallardo, T., Brunini, A., 2008. *The Scattered Disk: Origins, Dynamics, and End States*, p. 259.
- Gunnarsson, M., Bockelée-Morvan, D., Biver, N., Crovisier, J., Rickman, H., 2008. Mapping the carbon monoxide coma of comet 29P/Schwassmann-Wachmann 1. *Astron. Astrophys.* 484, 537. <https://doi.org/10.1051/0004-6361:20078069>.
- Hoskins, W.A., Aadland, R.S., Meckel, N.J., Talerico, L.A., Monheiser, J.M., 2007. NEXT ion propulsion system production readiness. In: *43rd AIAA/ASME/SAE/ASEE Joint Propulsion Conference & Exhibit* (abstract).
- Ivanova, A., Korsun, P., Afanasiev, V., 2015. C/2002 VQ94 (LINEAR) and 29P/Schwassmann-Wachmann 1 – CO+ and N2+ rich comets. In: *Highlights of Astronomy*, 16, p. 159. <https://doi.org/10.1017/S1743921314005146>, 159.
- Jewitt, D., 2009. The active Centaurs. *Astron. J.* 137, 4296. <https://doi.org/10.1088/0004-6256/137/5/4296>.
- Jewitt, D., Agarwal, J., Hui, M.-T., Li, J., Mutchler, M., Weaver, H., 2019. Distant comet C/2017 K2 and the cohesion bottleneck. *Astron. J.* 157, 65. <https://doi.org/10.3847/1538-3881/aaf38c>.
- Laine, S., et al., 2020. Spitzer observations of the predicted Eddington flare from Blazar OJ 287. *Astrophys. J.* 894, L1. <https://doi.org/10.3847/2041-8213/ab79a4>.
- Lauer, T.R., et al., 2021. New Horizons observations of the cosmic optical background. *Astrophys. J.* 906, 77. <https://doi.org/10.3847/1538-4357/abc881>.
- Luu, J.X., Jewitt, D.C., 1990. Cometary activity in 2060 Chiron. *Astron. J.* 100, 913. <https://doi.org/10.1086/115571>.
- Marcialis, R.L., Buratti, B.J., 1993. CCD photometry of 2060 Chiron in 1985 and 1991. *Icarus* 104, 234. <https://doi.org/10.1006/icar.1993.1098>.
- Matsuura, S., et al., 2017. New spectral evidence of an unaccounted component of the near-infrared extragalactic background light from the CIBER. *Astrophys. J.* 839, 7. <https://doi.org/10.3847/1538-4357/aa6843>.
- Meech, K.J., et al., 2009. Activity of comets at large heliocentric distances pre-perihelion. *Icarus* 201, 719. <https://doi.org/10.1016/j.icarus.2008.12.045>.
- Mosher, D., 2017. NASA Could Run Out of Nuclear Fuel for Deep-Space Missions within a Decade. *Business Insider*.
- Murphy, D.M., Eskenazi, M.L., McEachen, M.E., Spink, J.W., 2016. UltraFlex and MegaFlex – advancements in highly scalable solar power. In: *3rd AIAA Spacecraft Structures Conference*, 1947. <https://doi.org/10.2514/6.2016-1947>.
- Nesvorný, D., et al., 2019. OSSOS. XIX. Testing early Solar System dynamical models using OSSOS Centaur detections. *Astron. J.* 158, 132. <https://doi.org/10.3847/1538-3881/ab3651>.
- NRC, 2003. *New Frontiers in the Solar System: an Integrated Exploration Strategy*. The National Academies Press, Washington, DC. <https://doi.org/10.17226/10432>.
- NRC, 2008. *Opening New Frontiers in Space: Choices for the Next New Frontiers Announcement of Opportunity*. The National Academies Press, Washington, DC. <https://doi.org/10.17226/12175>.

- NRC, 2011. Vision and Voyages for Planetary Science in the Decade 2013-2022. The National Academies Press, Washington, DC. <https://doi.org/10.17226/13117>.
- Olkin, C.B., et al., 2021. Lucy mission to the Trojan asteroids: concept of operations and instrumentation. *Planet Sci. J.* (accepted manuscript).
- Ortiz, J.L., et al., 2015. Possible ring material around centaur (2060) Chiron. *Astron. Astrophys.* 576 <https://doi.org/10.1051/0004-6361/201424461>.
- Pätzold, M., et al., 2019. The nucleus of comet 67P/Churyumov-Gerasimenko - part I: the global view - nucleus mass, mass-loss, porosity, and implications. *Mon. Not. Roy. Astron. Soc.* 483, 2337. <https://doi.org/10.1093/mnras/sty3171>.
- Peixinho, N., et al., 2020. From Centaurs to comets - 40 years. In: Prialnik, D., Barucci, M.A., Young, L.A. (Eds.), *The Trans-neptunian Solar System*. Elsevier, Amsterdam, Netherlands, pp. 307–330. <https://doi.org/10.1016/b978-0-12-816490-7.00014-x>.
- Prialnik, D., Brosch, N., Ianovici, D., 1995. Modelling the activity of 2060 Chiron. *Mon. Not. Roy. Astron. Soc.* 276, 1148. <https://doi.org/10.1093/mnras/276.4.1148>.
- Reuter, D.C., et al., 2008. Ralph: a visible/infrared imager for the New Horizons Pluto/Kuiper belt mission. *Space Sci. Rev.* 140, 129–154.
- Romon-Martin, J., Delahodde, C., Barucci, M.A., de Bergh, C., Peixinho, N., 2003. Photometric and spectroscopic observations of (2060) Chiron at the ESO very large telescope. *Astron. Astrophys.* 400, 369–373. <https://doi.org/10.1051/0004-6361:20021890>.
- Ruprecht, J.D., et al., 2015. 29 November 2011 stellar occultation by 2060 Chiron: symmetric jet-like features. *Icarus* 252, 271–276. <https://doi.org/10.1016/j.icarus.2015.01.015>.
- Senay, M.C., Jewitt, D., 1994. Coma formation driven by carbon monoxide release from comet Schwassmann-Wachmann 1. *Nature* 371, 229. <https://doi.org/10.1038/371229a0>.
- Sicardy, B., et al., 2020. The dynamics of rings around Centaurs and Trans-Neptunian objects. In: Prialnik, D., Barucci, M.A., Young, L.A. (Eds.), *The Trans-neptunian Solar System*. Elsevier, Amsterdam, Netherlands, pp. 249–270. <https://doi.org/10.1016/b978-0-12-816490-7.00011-4>.
- Sickafoose, A.A., et al., 2020. Characterization of material around the centaur (2060) Chiron from a visible and near-infrared stellar occultation in 2011. *Mon. Not. Roy. Astron. Soc.* 491, 3643. <https://doi.org/10.1093/mnras/stz3079>.
- Stern, S.A., et al., 2015. The Pluto system: initial results from its exploration by new horizons. *Science* 350 id.aad1815.
- Stern, S.A., et al., 2009. LRO LAMP: experiment description, observation status, and early results, 41, 26, 08 (abstract).
- Stern, S.A., et al., 2019. Initial results from the New Horizons exploration of 2014 MU69, a small Kuiper belt object. *Science* 364. <https://doi.org/10.1126/science.aaw9771>.
- Stern, S. Alan, Slater, David C., Scherrer, John, Stone, John, Dirks, Greg, Versteeg, Maarten, Davis, Michael, Gladstone, G. Randall, Parker, Joel W., Young, Leslie A., Siegmund, Oswald H.W., et al., 2008. ALICE: the ultraviolet imaging spectrograph aboard the New Horizons Pluto-Kuiper belt mission. *Space Sci. Rev.* 140, 155. <https://doi.org/10.1007/s11214-008-9407-3>.
- Tedesco, E.F., Noah, P.V., Noah, M., Price, S.D., 2004. Iras Minor Planet Survey v6.0. NASA Planetary Data System, IRAS-A-FPA-3-RDR-IMPS-V6.0.
- Wierzchos, K., Womack, M., Sarid, G., 2017. Carbon monoxide in the distantly active Centaur (60558) 174P/Echeclus at 6 AU. *Astron. J.* 153, 230. <https://doi.org/10.3847/1538-3881/aa689c>.
- Womack, M., Stern, S.A., 1999. The detection of carbon monoxide gas emission in (2060) Chiron. *Sol. Syst. Res.* 33, 187.
- Zemcov, M., et al., 2018. Astrophysics with new horizons: making the most of a generational opportunity. *Publ. Astron. Soc. Pac.* 130, 115001. <https://doi.org/10.1088/1538-3873/aadb77>.